



ELSEVIER

Journal of Chromatography A, 721 (1996) 203–212

JOURNAL OF  
CHROMATOGRAPHY A

## Solution properties of polyelectrolytes XII.<sup>☆</sup> Semi-quantitative approach to mixed electrostatic and hydrophobic polymer–gel interactions

Rosa García, Iolanda Porcar, Juan E. Figueruelo, Vicente Soria, Agustín Campos\*

*Departament de Química Física, Universitat de València, E-46100 Burjassot, València, Spain*

First received 17 May 1995; revised manuscript received 22 June 1995; accepted 4 July 1995

### Abstract

Aqueous size-exclusion chromatography of polyanions, where secondary effects affect the total separation mechanism, was investigated. For elution of polyelectrolytes on inorganic silica-based supports, the electrostatic polymer–gel repulsive interactions were evaluated through the values for a hypothetical repulsion layer,  $X_e$ , according to the model developed by other workers. Using a similar procedure, the existence of an effective barrier defined as  $X_e - X_h$  is proposed for those systems in which electrostatic repulsion and hydrophobic interactions take place simultaneously as secondary mechanisms.  $X_h$  can be viewed as a measure of the “enlargement” of the geometrical pore radius due to reversible adsorption of polyanions in organic polymeric packings. In the light of the values of this effective barrier on the pore surface, the intensity and contribution of each type of solute–matrix interaction to the overall chromatographic process can be analysed as a function of polymer size and mobile phase composition, pH and ionic strength.

### 1. Introduction

Aqueous size-exclusion chromatography (ASEC) has attracted increasing attention in recent years because of the possibilities it offers both in basic biochemistry and for biotechnological applications. It has proved to be a powerful tool in the separation and characterization of biopolymers (peptides, proteins, etc.) [1–6] and macromolecular assemblies (viral particles, liposomes, etc.) [7,8], using typically mild, non-ag-

gressive mobile phase conditions which preserve the native structure and functionality of the solute.

Pure or “ideal” ASEC requires that the chromatographic separation is governed exclusively according to the hydrodynamic properties of the solute. However, considerable experimental evidence has shown that the elution mechanism of most polyions and biopolymers on ASEC packings deviates from a pure size-exclusion mechanism, mainly owing to the diverse nature of the so-called secondary effects, including ion exclusion and ion exchange, hydrophobic interaction and hydrogen bonding, originating from specific solute–matrix interactions [9].

At present, the available hydrophilic gels

<sup>☆</sup> For Part XI, see Ref. [22]. Paper presented at the *XXVth Annual Meeting of the Spanish Chromatography Group*, 7<sup>th</sup> as *Jornadas de Análisis Instrumental*, Madrid, 3–6 April, 1995.

\* Corresponding author.

exhibit surface residual charges which interact with like-charged polyions preventing the elution mechanism from being “ideal”. Abundant reports on the secondary effects in ASEC demonstrate that these effects occur for both organic and inorganic supports [2,10–23]. Although these effects have turned out to be advantageous in some instances [24] and have been exploited to improve the separation of macromolecules of similar hydrodynamic volume, it is in general desirable to minimize or cancel them, particularly for characterization purposes. Considerable efforts have been made in this direction both by manufacturers, to design supports that are as inert as possible, and by chromatographers, to use appropriate mobile phase conditions. At the same time, different theoretical approaches have been elaborated attempting to quantify the aforementioned secondary effects. However, it seems that total suppression of these effects has not yet been achieved and that there is no theory capable of predicting them in a completely satisfactory manner. For this reason, most attempts to account for secondary mechanisms are based on experimental data obtained on packing materials of very diverse nature with model charged macromolecules.

Dubin and co-workers [11,12,25] proposed a model to predict ion-exclusion effects based on the reduction in the pore volume accessible to polyions as a function of the electrostatic potential of the stationary phase. They also proposed [26] the use of a hydrophobicity index related to the hydrophobic effect. Mori [15] established an empirical correlation between the repulsion volume and eluent ionic strength. Styring et al. [13] focused on the electrostatic behaviour of the ionic atmosphere surrounding the polyelectrolyte without paying attention to the residual charge of the gel. Some theoretical models for ion-exclusion have been reported, most of them based on the Poisson–Boltzmann equation [27,28]. Finally, Dubin’s group has reviewed with experimental data several models on SEC behaviour [29]. However, so far there has been no rigorous theoretical treatment of hydrophobic interactions in ASEC of polyions. Our group has recently proposed a semi-quantitative approach in the framework of the Flory–Huggins theory in terms of polymer–gel matrix compatibility [22].

titative approach in the framework of the Flory–Huggins theory in terms of polymer–gel matrix compatibility [22].

In contrast with the elution mechanism of neutral polymers in organic media [30], the understanding of the global separation process of hydrophilic ionic polymers and biopolymers in aqueous media demands much more theoretical and experimental work.

In this paper, we present an empirical approach to calculate the barrier on the pore surface forbidden to solute permeation when both repulsive electrostatic and hydrophobic interactions take place simultaneously. The procedure is based on that developed by Dubin et al. [12] for electrostatic interactions exclusively. The results are discussed as a function of the chemical nature of both polyion and support and also the pH and ionic strength of the mobile phase.

## 2. Theory

The elution volume of an uncharged polymer,  $V_e$ , can be expressed as a function of the partition coefficient in SEC through the conventional equation

$$V_e = V_0 + K_{SEC}^n V_p \quad (1)$$

where  $V_0$  is the interstitial volume,  $V_p$  is the pore volume and  $K_{SEC}^n$  the partition or distribution coefficient accounting for the pore volume fraction available to the neutral polymeric solute. Based on this concept, a theoretical expression for  $K_{SEC}^n$  was derived [31]:

$$\begin{aligned} K_{SEC}^n &= \frac{V_e - V_0}{V_p} = \frac{\text{available pore volume}}{\text{total pore volume}} \\ &= \frac{\text{volume of pores with radius larger than the solute radius}}{\text{total pore volume}} \\ &= \frac{n\bar{l}\pi(a_p - R_\eta)^2}{n\bar{l}\pi a_p^2} = \left(\frac{a_p - R_\eta}{a_p}\right)^2 \quad (2) \end{aligned}$$

if a cylindrical geometry for the pores is assumed, and it has been found that it provides good fits for SEC data for neutral polymers in

several stationary phases [2,14,25,32]. In Eq. 2,  $n$  and  $\bar{l}$  are the number and the mean length of pores, respectively,  $a_p$  is the mean pore radius given by the manufacturer and  $R_\eta$  is the hydrodynamic radius of the macromolecule.  $R_\eta$  is related to the hydrodynamic volume or solute size,  $M[\eta]$ , by

$$R_\eta = \left( \frac{3 \cdot 10^{23} M[\eta]}{\pi N_A} \right)^{1/3} \quad (3)$$

where the intrinsic viscosity,  $[\eta]$ , is expressed in ml/g and  $R_\eta$  in Å.

The deduction of Eq. 2 allows us to write any expression for the partition coefficient even if the main separation mechanism is not exclusively pure size exclusion. In this regard, when other secondary mechanisms are involved in the chromatographic separation process as a consequence of polymer–packing interactions (mainly electrostatic and hydrophobic), we can deduce similar expressions to Eqs. 1 and 2, as we shall see later.

Let us now describe in terms of elution volume and partition coefficient the most characteristic secondary effects in ASEC. First, we shall treat the electrostatic repulsion alone, and second, both electrostatic and hydrophobic interactions taking place simultaneously.

### 2.1. Electrostatic repulsion as a secondary effect

This non-size-exclusion mechanism occurs, for instance, in the ASEC of polyanions permeating through silica-based packings [10–21]. In these cases, the elution volume of a charged polymer or polyelectrolyte can be defined as

$$V'_e = V_0 + K'_{SEC} K V_p \quad (4)$$

where  $V'_e < V_e$  for a given hydrodynamic volume (or macromolecular size) and  $K'_{SEC}$  and  $K$  are the partition coefficients accounting for size exclusion (obtained experimentally from the polyelectrolyte calibration graph) and for secondary mechanisms, in this case exclusively an ion-exclusion effect, respectively. Now, we can include this effect either in a unique coefficient,  $K'_{SEC}$ , or in the value of the total pore volume,  $V'_p$ :

(a) Assuming a unique value for the partition coefficient, Eq. 4 can be written as

$$V'_e = V_0 + K'_{SEC} V_p \quad (5)$$

where  $K'_{SEC} = K'_{SEC} K$ .

(b) The inclusion of  $K$  in the pore volume leads to

$$V'_e = V_0 + K'_{SEC} V'_p \quad (6)$$

where  $V'_p = K V_p$ . Later we shall demonstrate that Eqs. 5 and 6 are both equivalent for describing the elution behaviour of polyelectrolytes.

In the light of the first assumption,  $K'_{SEC}$  given in Eq. 5 can be expressed by analogy with Eq. 2 as

$$K'_{SEC} = \frac{V'_e - V_0}{V_p} = \left( \frac{a_p - X_e - R_\eta}{a_p} \right)^2 \quad (7)$$

where  $X_e$  is the thickness of the barrier inside the pore forbidden to the polyanion permeation owing to electrostatic repulsion [12] or as a “repulsion length” [25].

Alternatively, the second assumption (Eq. 6) gives

$$K'_{SEC} = \frac{V'_e - V_0}{V'_p} = \left( \frac{a_p - X_e - R_\eta}{a_p - X_e} \right)^2 \quad (8)$$

It is important to note that both  $K'_{SEC}$  (Eq. 2) and  $K'_{SEC}$  (Eq. 8) account for distribution coefficients due to size exclusion, but each one is defined from the concepts of available and total pore volume in their respective calibration graphs.

In order to study in greater depth the physical meaning of  $X_e$  and following the model depicted by Dubin et al. [12], we can find an expression for the difference in the elution volumes of a neutral and a charged polymer (subtracting Eqs. 1 and 5) with the same hydrodynamic size or  $R_\eta$ , but with different effective pore radius given by Eqs. 2 and 7, respectively. Then,

$$\begin{aligned} \Delta V_e &= V_e - V'_e = K'_{SEC} V_p - K'_{SEC} V_p \\ &= \frac{V_p}{a_p^2} (2a_p X_e - X_e^2 - 2X_e R_\eta) \end{aligned} \quad (9)$$

The same expression for  $\Delta V_e$  is reached from

Eqs. 2 and 8. As we shall see in the Results section, from Eq. 9 one can investigate whether there is any dependence of  $X_e$  on the polymer molecular mass.

On the other hand, it is interesting to find an expression to evaluate quantitatively the thickness of the electrostatic layer on the pore surface. Dubin et al. [12] proposed a procedure, that briefly is as follows: consider a neutral and a charged polymer that co-elute (both having the same elution volume) but each with their respective sizes,  $R_\eta$  and  $R'_\eta$ , and  $R_\eta > R'_\eta$ . Then, from the equality of Eqs. 1 and 5 it follows that  $K_{SEC}^n V_p = K_{SEC}^p V_p$ , where the partition coefficients are given by Eqs. 2 and 7 (in the latter, replacing  $R_\eta$  by  $R'_\eta$ ). Combining these equations one obtains

$$X_e = R_\eta - R'_\eta \quad (10)$$

In a similar way, equating Eqs. 1 and 6,  $K_{SEC}^n V_p = K_{SEC}^p V_p$  and substituting Eqs. 2 and 8 the same result for  $X_e$  is reached, as was pointed out by Dubin et al. [12], which demonstrates the validity of including the secondary effects either in the distribution coefficient or in the pore volume.

In conclusion, Eq. 10 is valid for evaluating the repulsion layer when electrostatic polymer-gel interactions are the only secondary mechanism besides pure size exclusion.

## 2.2. Electrostatic repulsion mixed with hydrophobic interaction as secondary effects

Both types of opposite polymer-gel interactions are present simultaneously, for instance, in the ASEC of polyanions in hydrophilic polymer-based supports [15,17,19–22] or in the SEC of proteins in anionic Superose packings [2].

We propose for these types of systems that follow non-ideal chromatographic behaviour an effective pore radius defined as  $a_p - (X_e - X_h)$  (instead of  $a_p - X_e$ ) as in the previous section, where only electrostatic repulsion was involved). The contribution of  $X_h$  to the pore radius arises from the attractive nature of the polymer-gel hydrophobic interactions, and can be viewed as an effective “enlargement” of the pore, that is,

as if the pore could be hypothetically larger than its geometrical size. For this particular case, Eqs. 5 and 6 can be rewritten as, respectively,

$$K_{SEC}' = \left[ \frac{a_p - (X_e - X_h) - R_\eta}{a_p} \right]^2 \quad (11)$$

and

$$K_{SEC}^p = \left[ \frac{a_p - (X_e - X_h) - R_\eta}{a_p - (X_e - X_h)} \right]^2 \quad (12)$$

Following the same procedure as before, the difference between the elution volumes of both neutral and charged polymers with the same hydrodynamic radius will now be

$$\Delta V_e = \frac{V_p}{a_p^2} [2a_p(X_e - X_h) - (X_e - X_h)^2 - 2(X_e - X_h)R_\eta] \quad (13)$$

irrespective of using Eqs. 2 and 11 or Eqs. 2 and 12.

As can be seen, Eq. 13 is more general than Eq. 9 since it takes into account not only electrostatic repulsions but also hydrophobic interactions. When the last type of interactions are not present, then  $X_h \rightarrow 0$  and Eq. 13 obviously becomes Eq. 9.

The calculation of this new effective layer surrounding the pore surface needs the same treatment as in the preceding section. Taking a neutral polymer and a polyelectrolyte with different sizes,  $R_\eta$  and  $R'_\eta$ , co-eluting ( $V_e = V'_e$ ) and by rearranging the appropriate equations (Eqs. 1 and 5 or 6, and Eqs. 2 and 11 or 12), it is derived that

$$X_e - X_h = R_\eta - R'_\eta \quad (14)$$

The values of the effective layer calculated through Eq. 14 denote that when  $R_\eta > R'_\eta$  (e.g. polyanion calibration graphs placed on the left-hand side of the reference graph), electrostatic repulsion will be the predominant secondary mechanism and  $X_e > X_h$ , whereas if the hydrophobic interaction is the main secondary effect (calibration graphs on the right), under given experimental conditions,  $R_\eta < R'_\eta$  and  $X_e < X_h$ .

### 3. Experimental

#### 3.1. Chemicals and reagents

The standards of neutral polymers used were dextran samples from Pharmacia (Uppsala, Sweden) with nominal molar masses of 10 000, 17 700, 40 000, 66 900, 83 300, 170 000, 500 000 and 2 000 000 g mol<sup>-1</sup>, and poly(ethylene oxide) (PEO) from Fluka (Darmstadt, Germany) of 2000 and 4000 g mol<sup>-1</sup>. The polyelectrolytes used as charged polymers were poly(L-glutamic acid) (PGA) from Sigma (St. Louis, MO, USA) and sodium poly(styrene sulphonate) (PSS) from Pressure Chemical (Pittsburgh, PA, USA). Their nominal molar masses were 13 600, 43 000 and 77 800 g mol<sup>-1</sup> for PGA and 1600, 16 000, 31 000, 88 000 and 177 000 g mol<sup>-1</sup> for PSS.

The solvents employed for viscometric measurements and as eluents in ASEC were buffers made up from NaH<sub>2</sub>PO<sub>4</sub> and Na<sub>2</sub>HPO<sub>4</sub> for pH 7.0 and from NaOAc and HOAc for pH 4.0 and 5.0. The desired ionic strength was adjusted from 0.005 to 0.20 M. All reagents used in the preparation of buffers were of analytical-reagent grade from Merck (Darmstadt, Germany).

#### 3.2. Methods

Viscosity values for uncharged polymers in pure water at 25.0 ± 0.1°C were evaluated through their viscometric equations given in Ref. [17]. Viscosity measurements on polyelectrolyte samples at the same temperature were performed with an AVS 440 automatic Ubbelohde-type capillary viscometer from Schott Geräte

(Hofheim, Germany). All the data have been reported previously [16,19–21,33], in addition to the experimental conditions and procedure.

SEC measurements were carried out on a Waters liquid chromatographic equipment described elsewhere [19]. Three columns were used in this work, a silica-based Protein I-250 from Waters (Milford, MA, USA) and two organic polymer-based columns, Ultrahydrogel 250 (UHG-250) from Waters and a Spherogel TSK PW4000 from Beckman Instruments (Galway, Ireland). Their main characteristics are listed in Table 1. Experimental details and elution volume data have been reported elsewhere [19–21,33].

### 4. Results and discussion

According to the expressions developed in the Theory section, it is possible to investigate the dependence of  $X_e$  or  $X_e - X_h$  on the polymer molar mass. Thus, at constant hydrodynamic volume ( $\log M[\eta]$ ) a plot of  $\Delta V_e$  against  $R_\eta$  should give information about the behaviour of the effective barrier on the pore surface with the molecular mass at a given eluent composition, pH and ionic strength,  $I$ . Fig. 1 shows this plot for two systems, PSS–Protein I-250 in acetate buffer (pH 4.0,  $I = 0.02$  M) and PGA–UHG-250 in acetate buffer (pH 5.0,  $I = 0.02$  M). Polymer–gel interactions in the former system have exclusively an electrostatic nature, so the data should be described through Eq. 9, whereas Eq. 13 would be appropriate to account for the other system where both repulsive and hydrophobic

Table 1  
Characteristics of the ASEC columns used

Column	Packing material	Length (cm)	I.D. (mm)	$a_p$ (Å) <sup>a</sup>	$V_0$ (ml) <sup>b</sup>	$V_p$ (ml) <sup>c</sup>
Protein I-250	Derivatized silica gel	30	7.5	125	5.90	6.10
TSK PW4000	Hydroxylated polyether gel	30	7.5	250	5.15	5.25
UHG-250	Hydroxylated poly(methacrylate)-based gel	30	7.8	125	5.50	5.48

<sup>a</sup>  $a_p$  = Mean pore radius.

<sup>b</sup> Determined with blue dextran.

<sup>c</sup> Determined with <sup>2</sup>H<sub>2</sub>O.

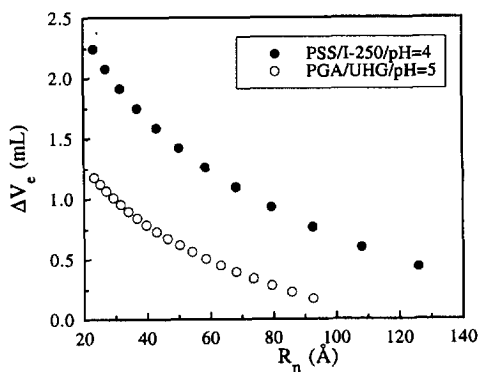


Fig. 1. Dependence of the difference in elution volumes between a neutral and a charged polymer on the hydrodynamic radius or polymer size (Eqs. 9 and 13) for two chromatographic systems: PSS in Protein I-250 gel at pH 4.0 and PGA in UHG-250 gel at pH 5.0. Eluent ionic strength  $I = 0.02 M$  in both cases.

effects are present. As can be seen,  $\Delta V_e$  does not decrease linearly with increasing  $R'_\eta$  in any case, which means that  $X_e$  or  $X_e - X_h$  is dependent on the sample molar mass injected. The same behaviour was also observed for all systems studied in this work.

In order to analyse in greater depth the dependence of  $X_e$  or  $X_e - X_h$  on the molecular mass, it is necessary to calculate the effective barrier through Eqs. 10 and 14, respectively. It is important to note that in all systems studied and calculations carried out, we obtained elution data for a large number of polymer sizes by interpolating within the primary experimental calibration graphs.

#### 4.1. PSS-Protein I-250

Fig. 2 shows plots of the thickness of the repulsion layer,  $X_e$ , as a function of  $R'_\eta$ , according to Eq. 10, for a typical system where only electrostatic repulsion can be considered as a secondary mechanism because of the inorganic nature of the silica gel used. Fig. 2a shows the variation of  $X_e$  for eluents with different pH values at constant  $I$ , and Fig. 2b corresponds to eluents of various  $I$  at a given pH. It is clearly seen that for a given value of  $I$  and  $R'_\eta$ ,  $X_e$  increases with increasing eluent pH, which can

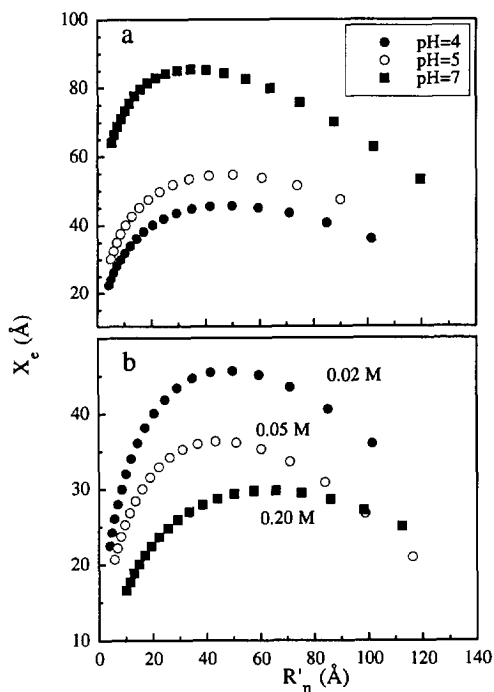


Fig. 2. Dependence of the electrostatic repulsion layer of the pore surface,  $X_e$ , on the equivalent polyion size represented by  $R'_\eta$  according to Eq. 10 for the system PSS in Protein I-250 packing and different mobile phases: (a)  $I = 0.02 M$  and pH (●) 4, (○) 5 and (■) 7; (b) pH 4.0 and  $I =$  (●) 0.02, (○) 0.05 and (■) 0.20  $M$ .

be easily understood. As the pH is raised, the extent of dissociation of the ionizable groups on the polymer chain and on the gel surface is also greater, increasing the repulsive forces between like charges (see Fig. 2a). The same effect is observed for a given  $R'_\eta$  and pH (Fig. 2b) as the eluent ionic strength is diminished, as a consequence of the lower screening of charges by counter ions.

The general trend of the curves accounting for the dependence of  $X_e$  on  $R'_\eta$  is the same under any conditions. At low values of  $R'_\eta$ ,  $X_e$  (or, more exactly, the first slope of the graph) increases markedly, reaching a "plateau" at intermediate values of  $R'_\eta$ , the width of which is higher at low pH and high  $I$  values, and decreasing finally as the polymer size approaches the value of the geometrical pore volume. The values of  $X_e$  are a measure of the ion-exclusion

effect. This behaviour is in agreement with other experimental results reported by Dubin et al. [12] on similar packings, and has also been explained theoretically through different models that take into account the polyion charge density [25].

Let us now analyse the dimensions of the effective layer,  $X_e - X_h$ , in those cases where the chromatographic separation is governed by size-exclusion, electrostatic repulsion or ion-exclusion and hydrophobic interactions. The calculations of  $X_e - X_h$  were conducted through Eq. 14, assuming that for a value of  $X_e - X_h > 0$  electrostatic repulsion is the predominant secondary mechanism whereas  $X_e - X_h < 0$  would mean important hydrophobic interaction. When both effects cancel each other, pure size exclusion takes place and the value of the aforementioned hypothetical barrier approaches zero.

#### 4.2. PGA in organic polymeric packings

Fig. 3 shows plots of Eq. 14 as a function of polymer molecular mass, represented by  $R'_\eta$ , for PGA in UHG-250 at pH (a) 7.0 and (b) 5.0 and different values of mobile phase ionic strength in the range 0.005–0.20 M. From a quantitative point of view, the effect of pH is as explained for Fig. 2. As expected, the values of  $X_e - X_h$  at a certain  $R'_\eta$  and  $I$  are always larger at pH 7.0 than 5.0.

At this point, the most important feature is to analyse the intensity of each type of interaction as the ionic strength is changed. The general trend of the curves depicted in Fig. 3 is different from that in the preceding section. At low  $I$ , the value of  $X_e - X_h$  is high at low molecular mass, which means that electrostatic repulsion is more intense when the polymer behaves as an oligomer with high charge density and rod-like conformation. As the polymer size increases, the magnitude of the hydrophobic interaction, represented by the value of  $X_h$ , becomes more and more important, increasing with size without reaching a "plateau". A possible explanation could be that, as the polymer chain increases, so also does the extent of apolar zones, raising the

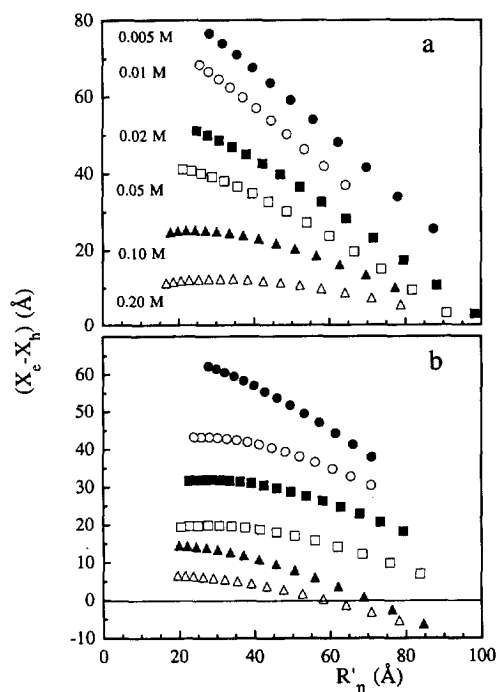


Fig. 3. Variation of the effective barrier on the pore surface ( $X_e - X_h$ ) with the equivalent polyion size represented by  $R'_\eta$  according to Eq. 14 for the system PGA in UHG-250 packing and eluents: (a) phosphate buffer (pH 7.0); (b) acetate buffer (pH 5.0). Ionic strength as shown.

possibility of hydrophobic interaction with the non-polar domains of the gel surface.

As the mobile phase ionic strength is increased, the curves of  $X_e - X_h$  vs.  $R'_\eta$  change less dramatically. On the one hand, the effect of  $I$  on the electrostatic repulsive force represented by  $X_e$  is to diminish it by counter-ion screening. As a consequence, the polyion conformation changes from rigid or stretched rod to random coil. On the other hand, this conformational change affects the hydrophobic interaction by decreasing it as well, because of an important number of non-polar areas in the polymer chain are hidden in the Gaussian coil structure.

Under the optimum-chromatographic conditions for this system (see Fig. 3b, lowest pH and highest  $I$ ), it is seen that the value of  $X_e - X_h$  is almost constant over all the range of molar masses studied, and approaches zero, which would mean an absence or balance of secondary

effects and a pure size-exclusion separation mechanism. Only at high polymer size does the effective barrier on the pore reach negative values, denoting a preponderance of hydrophobic solute–matrix interactions.

If one compares the dependence of  $X_e - X_h$  on  $R'_\eta$  with that of  $X_e$ , under the same experimental conditions, then although both magnitudes decrease with increase in polymer size, the former does so more dramatically. In other words, the increase in  $X_h$  with  $R'_\eta$  is higher than the decrease in  $X_e$ , as is reflected from the last slope of the curves (see Figs. 2 and 3).

The effect of pH on the values of the effective barrier shown in Figs. 2 and 3 is general for the rest of the systems studied here. For this reason, we shall show plots of Eq. 14 for systems which deserve some kind of comparison (different polyanion or gel) only at pH 5.0, avoiding unnecessary repetition of graphs at other pH values.

Fig. 4 depicts plots of Eq. 14 for PGA in TSK PW4000 gel at pH 5.0 and different values of the eluent ionic strength. The general trend observed is a diminution in the thickness of the barrier,  $X_e - X_h$ , as the polymer size is increased (at a given  $I$ ) and as the ionic strength is raised (for a certain value of  $R'_\eta$ ). Quantitatively, and for the sake of comparison with the preceding system, it is noted that at low  $I$  (0.005 M) the value of  $X_e - X_h$  is about 50 Å in TSK PW4000

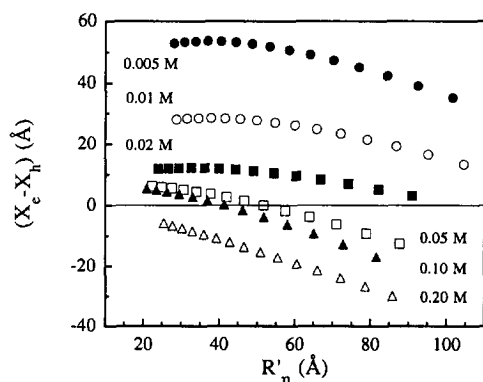


Fig. 4. Variation of the effective barrier on the pore surface ( $X_e - X_h$ ) with the equivalent polyion size represented by  $R'_\eta$  according to Eq. 14 for the system PGA in TSK PW4000 packing in an eluent of pH 5.0 and ionic strength as shown.

gel whereas on UHG-250 is ca. 60 Å (for low  $R'_\eta$ ). At the highest  $I$  (0.20 M), the barrier on the TSK gel is always negative, hence  $X_h > 0$ , which means that this gel is more “hydrophobic” than the other one. This behaviour is reasonable since, on the one hand, UHG-250 gel displays less apolar zones than TSK gel and, on the other, it has a higher percentage of ionizable groups per area unit, that is, a larger surface charge density. Therefore, on TSK PW4000 gel the appearance of salt-induced matrix–solute hydrophobic interactions is more plausible and the balance or suppression of secondary effects is achieved at intermediate ionic strength and more moderate experimental conditions in this gel.

#### 4.3. PSS in organic polymeric packings

Fig. 5 shows plots of Eq. 14 for the system of PSS in UHG-250 gel at pH 5.0 and diverse eluent ionic strength. In general the curves follow the same behaviour. At low  $I$  and  $R'_\eta$ , there is a rapid increase in  $X_e - X_h$ , then the values reach a “plateau” and decrease with increasing polymer size. As  $I$  is raised, the electrostatic effect is diminished at the expense of increasing the value of  $X_h$  or the hydrophobic effect. Thus, at intermediate  $I$  values, such as 0.05 M, the thickness of the effective barrier approaches zero. High values of ionic strength in this gel ( $I = 0.10$  and 0.20 M) lead to reversible

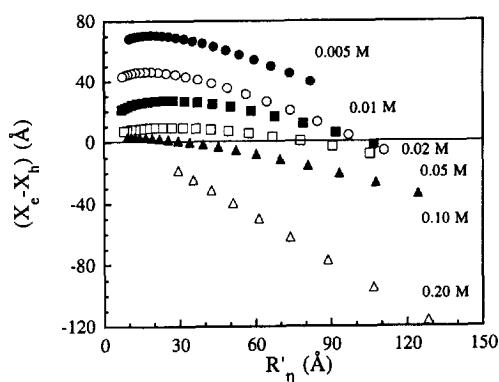


Fig. 5. Variation of the effective barrier on the pore surface ( $X_e - X_h$ ) with the equivalent polyion size represented by  $R'_\eta$  according to Eq. 14 for the system PSS in UHG-250 packing in an eluent of pH 5.0 and ionic strength as shown.



adsorption of the polymer, denoted by a positive value of  $X_h$  over all the range of molecular sizes studied, increasing markedly the hydrophobic interaction at  $I = 0.20 M$ .

A comparison of Figs. 5 and 3a from a quantitative point of view clarifies the influence of the type of polyanion on the  $X_e - X_h$  value. For instance, at a given  $R'_n$ , the value of  $X_e - X_h$  is always higher for PGA-UHG-250 than for PSS-UHG-250, irrespective of the eluent ionic strength, which would mean that PSS shows greater hydrophobic interaction with the same gel. Bearing in mind that at this pH (greater than the  $pK_a$  values of PGA and PSS) the ionic groups are dissociated to the same extent in both polymers, the intensity of the electrostatic repulsion or the value of  $X_e$  should be equivalent. Therefore, the only explanation for the different values of the  $X_e - X_h$  data obtained should be attributed exclusively to the intensity of the polymer-support hydrophobic interaction. The origin of this has to be necessarily the chemical nature of the polyion, since the observed adsorption of PSS on UHG-250 at high  $I$  (Fig. 5;  $X_h > 0$ ) occurs exclusively between the hydrocarbon patterns of the PSS (larger than those of PGA) and those of UHG gel packing. In this case, the polymer-gel attractive interaction becomes more intense owing to the unlocated nature of the driving forces involved affecting the overall domain of the macromolecule.

Finally, Fig. 6 shows plots of Eq. 14 for the system PSS in TSK PW4000 gel at pH 5.0 and different  $I$  values. On the one hand, at the lowest  $I$  (0.005 M), the same trend as in Fig. 5 is observed, at least in the range of sizes studied, indicating that the main secondary mechanism in the elution process will be ion exclusion. However, from a quantitative point of view, the value of  $X_e - X_h$  is always lower than the corresponding value in UHG-250 gel at any  $R'_n$  (see Fig. 5), hence even under these conditions hydrophobic interactions mixed with electrostatic interactions are present to some extent. On the other hand, only a small change in ionic strength (e.g., 0.01 M) causes a dramatic decrease in the  $X_e - X_h$  value which is negative over all the range of  $R'_n$ , or, in other words, a positive value

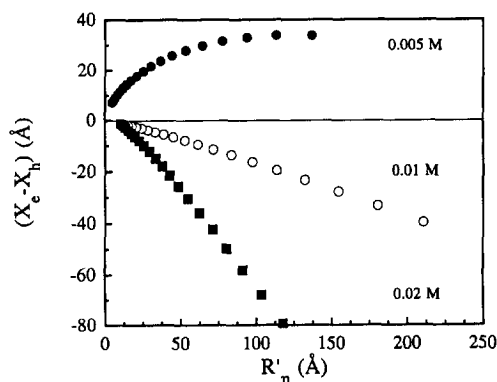


Fig. 6. Variation of the effective barrier on the pore surface ( $X_e - X_h$ ) with the equivalent polyion size represented by  $R'_n$  according to Eq. 14 for the system PSS in TSK PW4000 packing in an eluent of pH 5.0 and ionic strength as shown.

of  $X_h$  (“enlargement” of pore) increasing with polymer size and with ionic strength. The value of the effective barrier on the pore surface indicates that in this system there is a preponderance of hydrophobic interaction as a secondary mechanism over the global separation process. This behaviour is in agreement with the facts that PSS has more apolar zones than the other polyanion (PGA) and that TSK PW4000 gel is the most hydrophobic support of all those studied here, in chromatographic terms.

#### Acknowledgements

Financial support from the Dirección General de Investigación Científica y Técnica (Spain) under Grant No. PB91-0808 is gratefully acknowledged. One of the authors (I.P.) also thanks the Ministerio de Educación y Ciencia (Spain) for a long-term predoctoral fellowship.

#### References

- [1] K.M. Gooding and F.E. Regnier, in K.M. Gooding and F.E. Regnier (Editors), *HPLC of Biological Macromolecules* (Chromatographic Science Series, Vol. 51), Marcel Dekker, New York, 1990, Ch. 3.
- [2] P.L. Dubin, S.L. Edwards, M.S. Mehta and D. Tomalia, *J. Chromatogr.*, 635 (1993) 51.
- [3] P.L. Dubin, *Adv. Chromatogr.*, 31 (1992) 119.

- [4] C.G. Smith, P.B. Smith, A.J. Pasztor, Jr., M.L. Mckelvy, D.M. Meunier, S.W. Froelicher and A.S. Ellaboudy, *Anal. Chem.*, 65 (1993) 217R.
- [5] H.G. Barth and B.E. Boyes, *Anal. Chem.*, 64 (1992) 428R.
- [6] R.C. Montelaro, in P.L. Dubin (Editor), *Aqueous Size-Exclusion Chromatography (Journal of Chromatography Library, Vol. 40)*, Elsevier, Amsterdam, 1988, Ch. 10.
- [7] A. Foriers, B. Rombaut and A. Boeyé, *J. Chromatogr.*, 498 (1990) 105.
- [8] M. Ollivon, A. Walter and R. Blumenthal, *Anal. Biochem.*, 152 (1986) 262.
- [9] M. Janado and P.L. Dubin, in P.L. Dubin (Editor), *Aqueous Size-Exclusion Chromatography (Journal of Chromatography Library, Vol. 40)*, Elsevier, Amsterdam, 1988, Ch. 2 and 3.
- [10] M.G. Styring, C.J. Davison, C. Price and C. Booth, *J. Chem. Soc., Faraday Trans. 1*, 80 (1984) 3051.
- [11] P.L. Dubin and M.M. Tecklenburg, *Anal. Chem.*, 57 (1985) 275.
- [12] P.L. Dubin, C.M. Speck and J.I. Kaplan, *Anal. Chem.*, 60 (1988) 895.
- [13] M.G. Styring, H.H. Teo, C. Price and C. Booth, *Eur. Polym. J.*, 24 (1988) 333.
- [14] P.L. Dubin and J.M. Principi, *J. Chromatogr.*, 479 (1989) 159.
- [15] S. Mori, *Anal. Chem.*, 61 (1989) 530.
- [16] V. Soria, A. Campos, R. García, M.J. Parets, L. Braco and C. Abad, *J. Liq. Chromatogr.*, 13 (1990) 1785.
- [17] E. Pérez-Payá, L. Braco, C. Abad, V. Soria and A. Campos, *J. Chromatogr.*, 548 (1991) 93.
- [18] M. Potschka, *Macromolecules*, 24 (1991) 5023.
- [19] R. García, I. Porcar, A. Campos, V. Soria and J.E. Figueruelo, *J. Chromatogr. A*, 655 (1993) 191.
- [20] R. García, I. Porcar, A. Campos, V. Soria and J.E. Figueruelo, *J. Chromatogr. A*, 655 (1993) 3.
- [21] R. García, I. Porcar, A. Campos, V. Soria and J.E. Figueruelo, *J. Chromatogr. A*, 662 (1994) 61.
- [22] A. Campos, R. García, I. Porcar and V. Soria, *J. Liq. Chromatogr.*, 17 (1994) 3261.
- [23] B. Porsch and L.O. Sundelöf, *J. Chromatogr. A*, 669 (1994) 21.
- [24] P. Oroszlau, R. Blanco, X.M. Lu, D. Yarmush and B.L. Karger, *J. Chromatogr.*, 500 (1990) 481.
- [25] P.L. Dubin, R.M. Larter, C.J. Wu and J.I. Kaplan, *J. Phys. Chem.*, 94 (1990) 7243.
- [26] P.L. Dubin and J.M. Principi, *Anal. Chem.*, 61 (1989) 780.
- [27] G.F. Smith and W.N. Dean, *J. Colloid Interface Sci.*, 91 (1983) 571.
- [28] D.A. Hoagland, *Macromolecules*, 23 (1990) 2781, and references cited therein.
- [29] S. Hussain, M.S. Mehta, J.I. Kaplan and P.L. Dubin, *Anal. Chem.*, 63 (1991) 1132.
- [30] H.G. Barth and J.W. Mays (Editors), *Modern Methods of Polymer Characterization*, Wiley-Interscience, New York, 1991.
- [31] E.F. Casassa and Y. Tagami, *Macromolecules*, 2 (1969) 14.
- [32] H. Waldmann-Meyer, *J. Chromatogr.*, 410 (1987) 233.
- [33] R. García, Ph.D. Thesis, University of Valencia, 1992, Ch. 3 and 4.